Supporting Information

Dreyfus et al. 10.1073/pnas.0904439106

SI Materials and Methods

Construct Design, Protein Expression, and Purification. MtNAS was cloned, expressed, and purified as described by Dreyfus et al. (1). Briefly, the gene encoding MtNAS (MTH675) was cloned in pET101/D-TOPO to encode a protein fused with a C-terminal His tag. The expression plasmid was then transformed into the *E. coli* BL21 (DE3) strain to overexpress the recombinant protein. Selenomethionine-labeled protein was prepared as follows. BL21 *E. coli* cells expressing MtNAS were first incubated overnight at 37 °C in 10 mL LB medium. The cells were pelleted, washed in sterile water, and then resuspended in 1 L methionine-free medium (Molecular Dimensions) supplemented with 40 mg L-selenomethionine (SeMet), L-lysine, L-threonine, and L-phenylalanine, thus inhibiting the synthesis of methionine. When the culture reached an OD_{600} of 0.6–0.8, protein expression was induced by the addition of 1 mM IPTG overnight. The purification procedure for the selenomethionine-labeled protein was identical to that for wild-type protein. The addition of a reducing agent (to prevent the oxidation of selenomethionine) was omitted because it pushes the dimer:monomer ratio toward the monomeric form, which precludes further crystallization. The incorporation of SeMet was confirmed by MALDI MS. The yield of SeMet MtNAS was typically 2 mg/L culture, with a dimer:monomer ratio of ≈2:1.

Construction of Mutants. The previously constructed pET101-MtNAS plasmid containing the MtNAS cDNA was used as a template for site-directed mutagenesis using the QuikChange II XL Site-Directed Mutagenesis kit from Stratagene following the manufacturer's manual. For the mutant E81Q, the glutamic acid at position 81 was changed to glutamine by using a forward primer (5′-TCGGGATGAAGCTT**CAA**ATGGAAAAG-GCACAG-3′) and its reverse complement (mutation in bold). The same method was used to construct the mutant Y107F and the double mutant E81Q-Y107F using the following forward primer (5′-CTACTTCTACCCAAGG**TTC**C TTGAACTACT-TAA-3′) and its reverse complement. Expression and purification of mutants were done as previously described for MtNAS.

Crystallization and Data Collection. All of the crystallizations were done at 20 °C using the hanging drop vapor diffusion method. The best crystals of the native protein were obtained with 2 μL dimeric MtNAS solution mixed with an equal volume of reservoir solution containing 100 mM HEPES, pH 7.5, 22% (wt/vol) PEG3350, and 400 mM NaBr and equilibrated against 1 mL reservoir solution (1). Identical conditions were then used to obtain crystals from SeMet-labeled protein. These crystals have the same shape and correspond to the same crystal form. Crystals of the MtNAS-tNA-MTA and E81Q-Glu complexes were obtained by mixing purified protein solution (8 mg/mL) with equal volumes of the reservoir solution supplemented with 5 mM MTA or Glu, respectively. For the MtNAS-tNA-MTA crystals, the reservoir contained 100 mM HEPES, pH 7.5, 22% (wt/vol) PEG3350, 400 mM NaBr. For E81Q-Glu, the reservoir contained 100 mM Bis-Tris-propane, pH 8.5, 20% (wt/vol) PEG3350, 200 mM NaK-tartrate. The E81Q-SAM-Glu complex was obtained by soaking E81Q-Glu crystals in a drop containing reservoir solution and 5 mM SAM for 30 min prior flash-cooling.

Before data collection, crystals were soaked briefly in paraffin oil then flash-cooled directly in liquid nitrogen. All diffraction data were collected at the European Synchrotron Radiation Facility (ESRF; Grenoble, France). Data sets were processed with MOSFLM (2) and scaled using SCALA from the CCP4 suite (3, 4). All of the crystals belonged to space group $P2_12_12_1$ with slight variations in the unit cell parameters (see Table S1 for more details).

Crystal Structure Determination. The structure of the native dimeric protein was solved using selenomethionine-substituted protein and the MAD phasing method. Sixteen selenium positions were found using the program SOLVE (5). Using this phase information, 70% of the structural model was built automatically in RESOLVE (5). The model was extended to include a total of 265 residues out of 267 by manual building using Coot (6). Electron density is missing for the first methionine, the last residue, and for the His-tag. Several rounds of iterative model building and refinement were performed by using the program REFMAC (7). The high resolution MtNAS-tNA was solved by molecular replacement using the program MOLREP (8) and using the low resolution MtNAS-tNA from selenomethionine-labeled protein as the search model. After refinement with REFMAC, the *R*-factor of the final model is 20.0% (R_{free} = 23.6%; see Table S1), using all of the data from 44 to 1.7 Å resolution. The final model contains two molecules, two ligands (tNA molecules), two ions (assigned as bromide), and 507 solvent molecules.

The structure of the MtNAS-tNA-MTA complex was solved by molecular replacement with the MtNAS-tNA structure as the search model and refined at 1.66 Å resolution to an *R*-factor of 19.8% (R_{free} = 22.8%) (Table S1). The model contains amino acid residues 2–265, two tNA and two MTA molecules, two bromide ions, and 559 water molecules. Subsequently, the structures of the E81Q-Glu and E81Q-SAM-Glu complexes were solved by molecular replacement (Table S1) also with the MtNAS-tNA structure as the search model. The structure of the E81Q-Glu complex was refined at 2.3 Å resolution to an *R*-factor of 19.7% (R_{free} = 25.3%). The final model contains a dimer of MtNAS, two glutamic acid (one of which is clearly adopting an alternative conformation), and 724 solvent molecules. Data for the E81Q-Glu-SAM complex was refined to 2.5 Å (R = 19.3%; R_{free} = 27%). The final model contains a dimer of MtNAS, two SAM, one glutamic acid (based on molecule B, the electron density being difficult to interpret in molecule A), and 297 water molecules.

With an rms deviation below 0.9 Å, these monomers are almost identical, except for part of the N-terminal domain (residues 22–30). These differences in structure are mainly due to crystal packing. Graphics were generated by using the program PYMOL (www.pymol.org).

MS and tNA Synthase Activity. To confirm the identity of the additional molecule present in the native protein, noncovalent MS measurements were taken with a MicroTOF-Q (Bruker) equipped with an ESI source. The sample at a concentration of 10 μM in 50 mM ammonium acetate was continuously infused at a flow rate of 3 μL/min. The mass spectra were recorded in the 2,500–5,000 mass-to-charge (m/z) range. Data were acquired in the positive mode with calibration using a solution of 0.2 mg/mL CsI in water/isopropyl alcohol 1:1 (vol/vol).

An experiment was done in denaturing conditions to ensure correct molecule identification. MS/MS fragmentation was done directly on the eluting peptide (tNA). The concentration was 1 μM in water/acetonitrile 1:1 (vol/vol) with 0.2% formic acid and infused at a flow rate of 3 μL/min. The mass spectra were

recorded in the 50–3,000 m/z range. Using MS, we also confirmed that the purified mutant E81Q and double mutant E81Q/Y107F were empty and did not co-purify with tNA. The system was controlled with the software package MicroTOF control, and data were processed with DataAnalysis. Wild-type MtNAS (5 μM of the dimer in 20 mM Tris buffer, pH 9.0) and mutants activity were measured by following the production of tNA by MS. Samples were incubated for 30 min with 0.5 mM SAM and 0.5 mM glutamate at 25 °, 35 °, 45 °, and 55 °C. At 45 °C, samples were incubated for 60 min to observe the accumulation of tNA as a function of time.

1. Dreyfus C, Pignol D, Arnoux P (2008) Expression, purification, crystallization and preliminary X-ray analysis of an archaeal protein homologous to plant nicotianamine synthase. *Acta Crystallogr F* 64:933–935.
2. Leslie AGW (1993) in *Proceedings of the CCP4 Study Weekend: Data Collection and Processing*, eds Sawyer L, Isaacs N, Bailey S (SERC Daresbury Laboratory, Daresbury, UK), pp 44–51.
3. CCP4. (1994) The CCP4 suite: Programs for protein crystallography. *Acta Crystallogr D Biol Crystallogr* 50:760–763.
4. Evans PR (1997) *Scala*. *Joint CCP4 and ESF-EACBM Newsletter* 33:22–24.
5. Terwilliger TC (2003) SOLVE and RESOLVE: Automated structure solution and density modification. *Methods Enzymol* 374:22–37.
6. Emsley P, Cowtan K (2004) Coot: Model-building tools for molecular graphics. *Acta Crystallogr D Biol Crystallogr* 60:2126–2132.
7. Murshudov GN, Vagin AA, Dodson EJ (1997) Refinement of macromolecular structures by the maximum-likelihood method. *Acta Crystallogr D Biol Crystallogr* 53:240–255.
8. Vagin A, Teplyakov A (2000) An approach to multi-copy search in molecular replacement. *Acta Crystallogr D Biol Crystallogr* 56:1622–1624.
9. Diederichs K, Karplus PA (1997) Improved R-factors for diffraction data analysis in macromolecular crystallography. *Nat Struct Biol* 4:269–275.

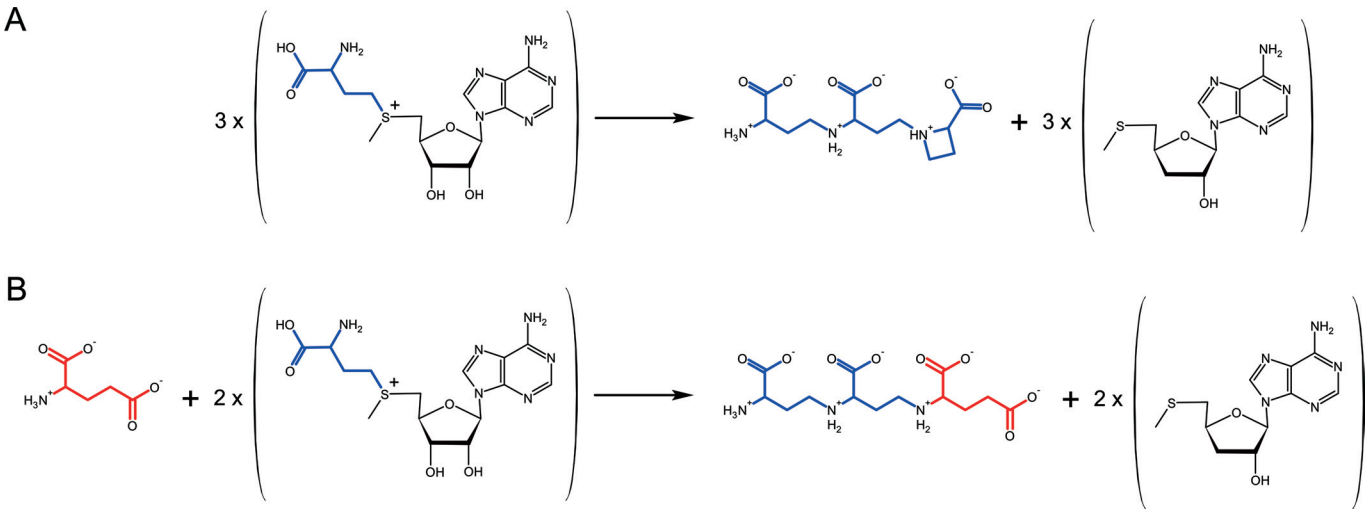

Fig. S1. Reaction scheme of NA (*A*) and tNA (*B*) synthesis. The aminopropyl moiety of SAM is colored in blue, and the glutamate is colored in red.

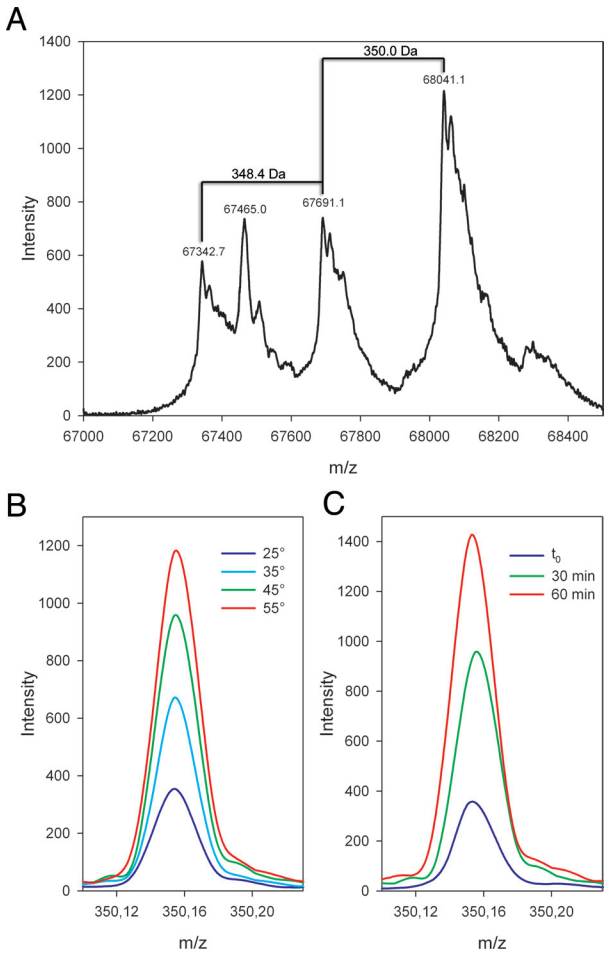

Fig. S2. Mass spectra of native dimeric MtNAS and in vitro accumulation of tNA as a function of temperature and time. (*A*) Noncovalent mass spectrum of as-prep dimers of MtNAS. The mass differences between the main peaks are indicated and suggest dimers coexist that are empty or loaded with one or two molecules of tNA (theoretical molecular weight of 350 Da). The second peak at 67,465.0 Da may correspond to a Tris adduct. (*B*) Accumulation of tNA as a function of temperature. Dimeric MtNAS was incubated 30 min with 0.5 mM SAM and 0.5 mM glutamate at different temperatures before MS. (*C*) Accumulation of tNA as a function of time at 45 °C with 0.5 mM SAM and 0.5 mM glutamate as the sole substrates.

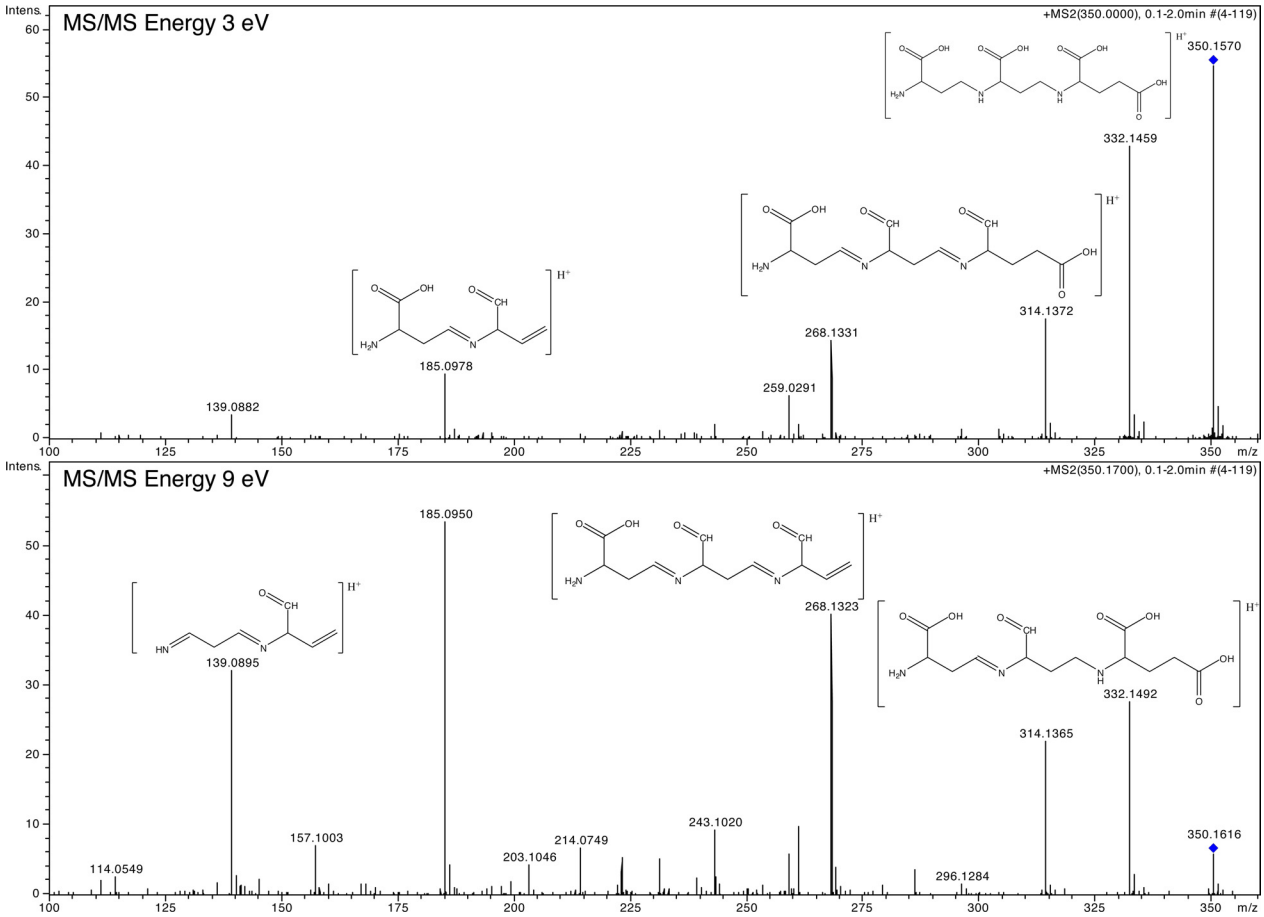

Fig. S3. Fragmentation of tNA at two different energies: (*A*) 3 eV and (*B*) 6 eV. Probable fragmentation scheme is given.

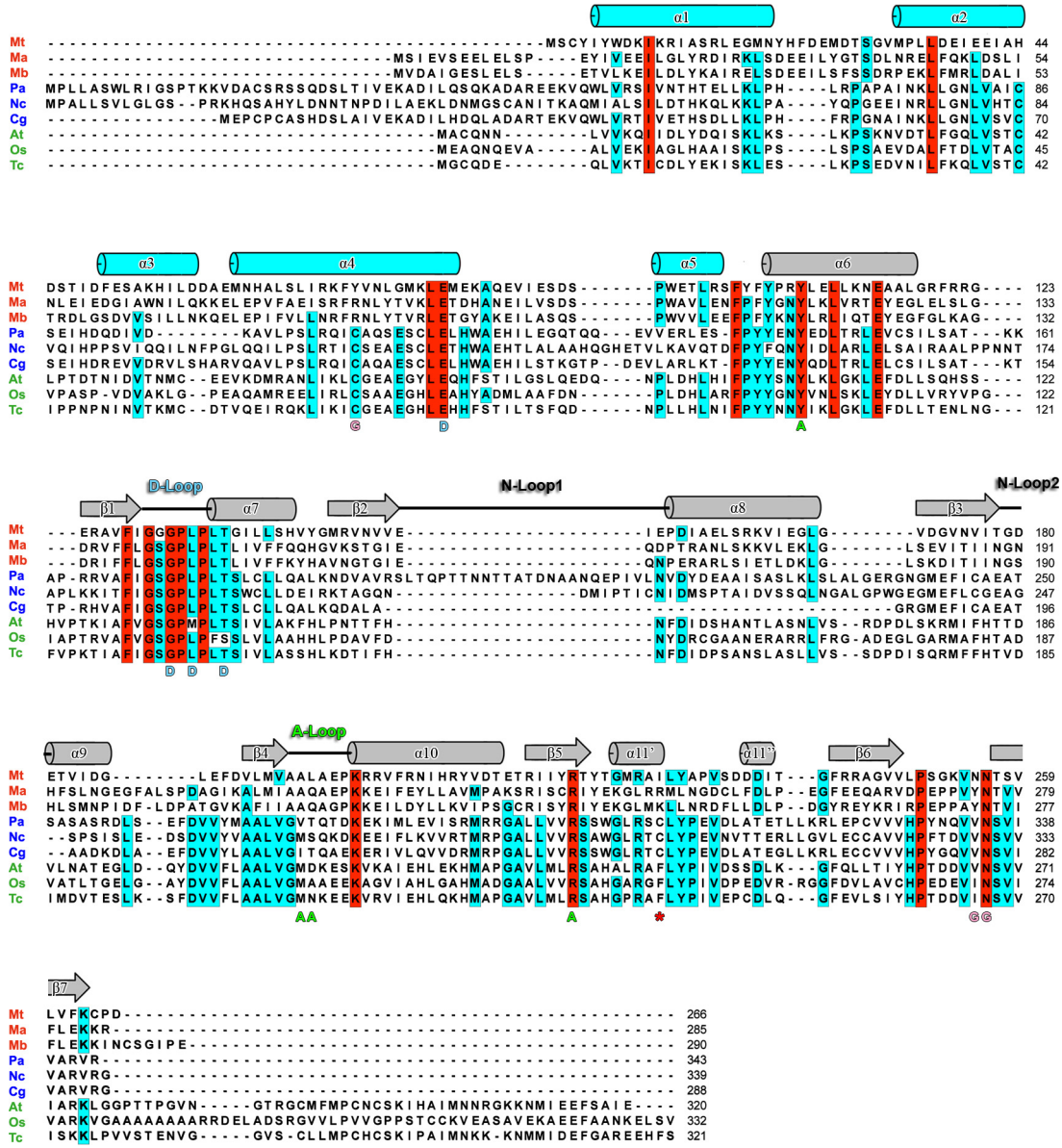

Fig. S4. Sequence alignment of three NAS from plants, three from fungi, and three from archaea. Identical residues are boxed in red, and a threshold of two-thirds is used (boxed in yellow) to highlight residues conserved in eukaryotes (plants and fungi) but not in archae. Features of the secondary structure of MtNAS are shown above the sequences with annotations below: (D) Residues hydrogen-bonded to the AP_1 moiety of tNA; (A) residues hydrogen-bonded to the AP_2 moiety of tNA; (G) residues hydrogen-bonded to the Glu_3 moiety of tNA; (*) position of the tomato *chloronerva* mutation that replaces a phenylalanine residue (F238) with a serine. Loops are named according to the role they play in the enzyme: D-Loop for donor loop, A-Loop for acceptor loop, and N-Loops for nucleotide loops. Mt, *Methanothermobacter thermautotrophicus* str. Delta H [Gene ID (GI), 1470636]; Ma, *Methanosarcina acetivorans* C2A (GI, 1475911); Mb, *Methanosarcina barkeri* str. Fusaro (GI, 3626156); Pa, *Podospora anserina* (GI, 27884573); Nc, *Neurospora crassa* OR74A (GI, 3874526); Cg, *Chaetomium globosum* CBS 148.51 (GI, 4394218); At, *Arabidopsis thaliana* (GI, 15238376); Os, *Oryza sativa* (GI, 108707744); Tc, *Thlaspi caerulescens* (GI, 27528464).

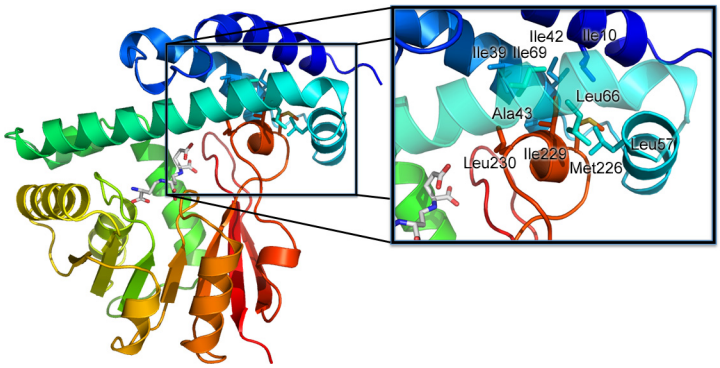

Fig. S5. Site of the mutation in the *chloronerva* mutant of tomato (*Lycopersicon esculentum*) in which phenylalanine 238 is replaced with a serine. The equivalent residue in MtNAS is isoleucine 229 localized in a hydrophobic ''hotspot'' that clearly contributes to the interaction, and probably the dynamics, between the N- and C-terminal domains.

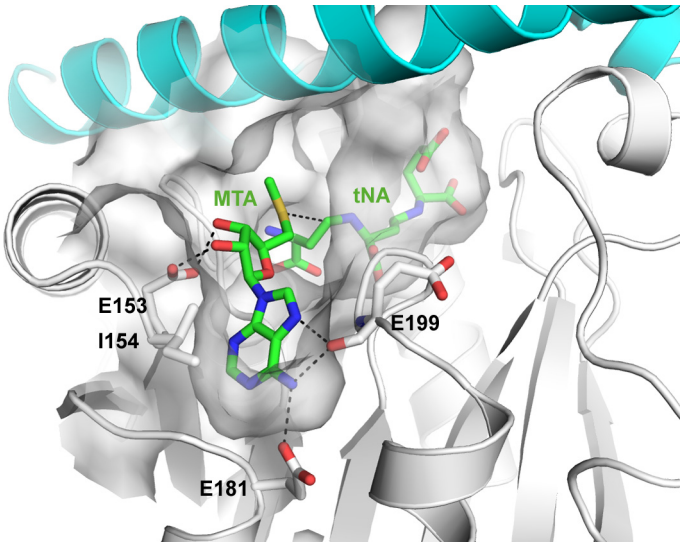

Fig. S6. Binding of the MTA molecule in the MtNAS-tNA-MTA ternary complex. Residues involved in the stabilization of MTA are shown as sticks.

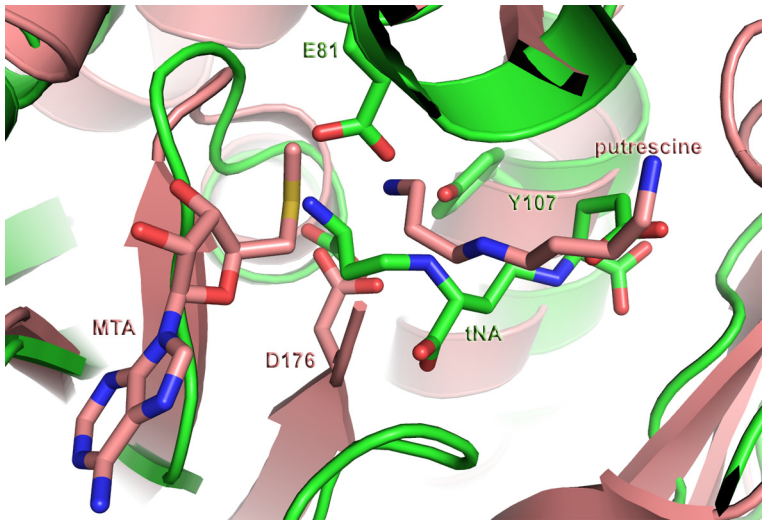

Fig. S7. Superimposition of the three-dimensional structures of MtNAS in complex with tNA (green), spermidine synthase in complex with spermine, and MTA (salmon; pdb code 2007). The catalytic residue of spermidine synthase (D176) is shown in stick form as well, as the residues playing a key role in tNA synthesis (E81 and Y107).

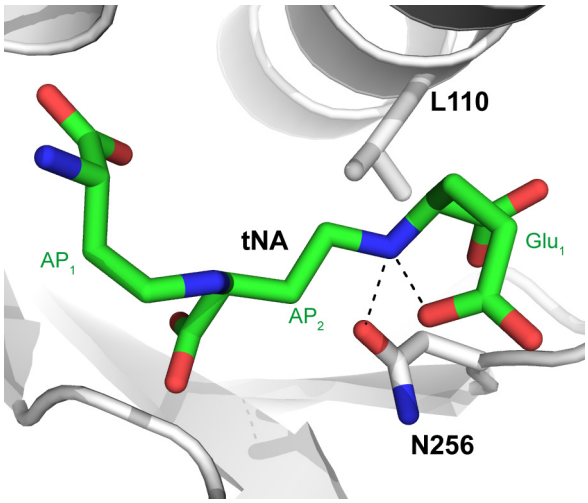

Fig. S8. The back of the reaction chamber selects secondary amines. The nitrogen atom of the Glu_1 moiety of tNA is involved in two hydrogen bonds (one intramolecular and one with Oε1 of N256). A primary amine would not be properly stabilized because of the presence of L110 side chain that prevents formation of an additional hydrogen bond with a primary amine.

A

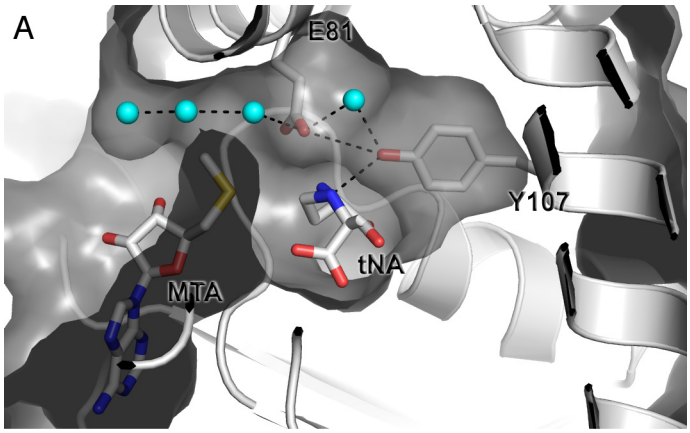

B

	tNA co-purification	tNA production
E81Q	-	+
Y107F	+	+
E81Q/Y107F	-	-

Fig. S9. Hydrogen-bond relay between residues and water molecules connecting the reaction chamber with the solvent. (*A*) Slab view of the proton wire that allows the release of the protons coming from the free amino group of the acceptors during the reaction. (*B*) Involvement of E81 and Y107 in the reaction mechanism. Both the single mutants are still able to produce tNA in vitro, and only the double mutant is completely deficient in tNA production. tNA co-purification was verified by MS. tNA production was followed by MS using purified protein and defined protein and substrates concentrations.

Table S1. Data collection, phasing and refinement statistics

Data Set	λ1	λ2	λ3	MtNAS-tNA	MtNAS-tNA-MTA	E81Q	E81Q-Glu	E81Q-SAM-Glu
PDB code				3FPE	3FPF	3FPG	3FPH	3FPJ
Data collection								
Beamlines	BM30			ID23–1	ID23–1	ID14–4	ID14–4	ID14–2
Space group	$P2_12_12_1$			$P2_12_12_1$	$P2_12_12_1$	$P2_12_12_1$	$P2_12_12_1$	$P2_12_12_1$
Cell dimensions								
a, Å	64.2	63.8	63.8	64.4	64.4	63,7	66.2	64.6
b, Å	68.3,	68.1,	68.1,	68.3,	68.7,	67.5,	69.8,	69.0,
c, Å	147.0	146.6	146.7	147.5	146.3	147.6	146.5	147.4
Wavelength, Å	0.98076	0.98064	0.97857	0.97920	0.97000	0.96850	0.96850	0.93300
Resolution Range, Å	34 - 2.00	34 - 2.00	34 - 2.00	44 - 1.70	44 - 1.66	68 - 2.00	70 - 1.80	30 - 1.80
High-resolution range, Å	2.18 - 2.00	2.18 - 2.00	2.18 - 2.00	1.79 - 1.70	1.75 - 1.66	2.11 - 2.00	1.9 - 1.80	1.9 - 1.80
Total observations	174,773	172,689	173,669	339,168	295,149	180,515	272,110	291,987
Unique reflections	44,331	43,742	43,785	71,075	76,848	36,210	61,535	61711
Completeness, %	99.6 (99.1)	99.7 (99.4)	99.7 (99.5)	98.5 (99.9)	99.3 (99.8)	83.9 (87)	97.4 (99.9)	99.8 (100)
$I/\sigma(I)$	21.1 (8.6)	20.5 (8.3)	19.4 (7.5)	12.4 (3.7)	13.2 (4)	13 (3)	16 (3)	15.6 (3.4)
R_{sym}, %	4.8 (14)	4.9 (14.6)	5.5 (17.9)	9.1 (33.7)	6.9 (28.2)	12.7 (55.4)	6.9 (46.8)	7.7 (37.6)
R_{pim},* %	4.6 (10.1)	4.1 (9.9)	4.1 (11.7)	5 (20.1)	3.9 (16.5)	6.2 (26.6)	3.7 (24.8)	4.4 (20.6)
R_{ano}, %	6.7 (11.9)	5.4 (10.9)	4.9 (12.4)					
No. of Se sites	16	16	16					
No. of methionine	20	20	20					
Refinement								
R_{cryst}/R_{free}, %				19.8 (23.3)	19.9 (22.9)	19.3 (25.6)	19.1 (24.6)	22.5 (28.4)
No. of atoms								
Protein				4,222	4,222	4,222	4,222	4,199
Water				507	559	542	724	540
tNA				48	48			
MTA					40			
Glu							20	Disordered
SAM								54
BTP						19		19
RMSD								
Bonds, Å				0.013	0.012	0.019	0.016	0.012
Angles, °				1.409	1.427	1.677	1.583	1.657
Average B factors, Å^2								
Protein				15.88	17.09	21.42	26.23	12.60
Water				24.88	26.21	37.38	39.17	24.66
tNA				16.46	13.74			
MTA					11.93			
Glu							30.78	Disordered
SAM								20.83
BTP						32.41		26.76

Values in parentheses are for the highest resolution shell. $R_{sym} = R_{merge} = \frac{\sum_{hkl}\sum_i |Ii(hkl) - \overline{I(hkl)}|}{\sum_{hkl}\sum_i Ii(hkl)}$. $R_{ano} = \frac{\sum_{hkl}||F_{PH}^+| - |F_{PH}^-||}{\sum_{hkl}\frac{|F_{PH}^+| + |F_{PH}^-|}{2}}$. $R_{cryst} = \frac{\sum|F_{obs} - F_{calc}|}{\sum F_{obs}}$.

R_{free} was calculated as for R_{cryst} but for 5% of the total reflections chosen at random and omitted from refinement.
*See ref. 9.